

# Shell structure of weakly-bound and resonant neutrons

Ikuko Hamamoto<sup>1,2</sup>

<sup>1</sup> *Division of Mathematical Physics,*

*Lund Institute of Technology at the University of Lund,*

*Lund, Sweden*

<sup>2</sup> *The Niels Bohr Institute,*

*Blegdamsvej 17, Copenhagen Ø,*

*DK-2100, Denmark*

## Abstract

The systematic change of shell structure in both weakly bound and resonant neutron one-particle levels in nuclei towards the neutron drip line is exhibited, solving the coupled equations derived from the Schrödinger equation in coordinate space with the correct asymptotic behaviour of wave functions for  $r \rightarrow \infty$ . The change comes from the behaviour unique in the one-particle motion with low orbital angular momenta compared with that with high orbital angular momenta. The observed deformation of very neutron-rich nuclei with  $N \gtrsim 20$  in the island of inversion is a natural result of this changed shell structure, while a possible deformation of neutron-drip-line nuclei with  $N \approx 51$ , which are not yet observed, is suggested.

PACS numbers: 21.60.Ev, 21.10.Pc, 27.30.+t, 27.50.+e

## I. INTRODUCTION

The study of one-particle motion in deformed potentials is the basis for understanding the structure of deformed drip-line nuclei. Since the Fermi level of drip line nuclei lies close to the continuum, both weakly-bound and positive-energy one-particle levels play a crucial role in the many-body correlation of those nuclei. Among an infinite number of one-particle levels at a given positive-energy, only some selected levels related to one-particle resonant levels will be important to bound states of drip-line nuclei. The motion of weakly-bound or low-energy resonant protons is not so different from that of well-bound protons except for very light nuclei, due to the presence of the Coulomb barrier. Therefore, the present talk is devoted to the change of shell structure of one-neutron levels.

The change of the shell structure in weakly-bound and resonant one-neutron levels is exhibited, which comes from the behavior unique in the one-particle motion with low orbital-angular-momenta ( $\ell$ ). For spherical shape the centrifugal barrier is absent for  $\ell=0$  orbits while the barrier is low for  $\ell=1$ . For deformed shape a given one-particle wave-function contains components with various  $\ell$  values, however, the minimum value of possible  $\ell$  for the wave-function components plays a crucial role in the present problem. For example, in the case of axially-symmetric quadrupole deformation  $\ell_{min}=0$  for  $\Omega^\pi = 1/2^+$  and  $\ell_{min}=1$  for both  $\Omega^\pi = 3/2^-$  and  $1/2^-$ , where  $\Omega$  expresses the component of the particle angular-momentum along the symmetry axis. For bound one-particle levels the  $\ell = 0$  component becomes always overwhelming in one-particle wave-functions with  $\Omega^\pi = 1/2^+$ , as the binding energy approaches zero. Namely, in the limit of small binding energy the halo phenomena which are created exclusively by the  $\ell = 0$  neutron wave-function appear for both spherical and deformed shapes. On the other hand, the decay of  $\Omega^\pi = 1/2^+$  one-particle resonances goes most easily through the  $s_{1/2}$  channel because of the absence of the centrifugal barrier. Therefore, it is in general difficult for an  $\Omega^\pi = 1/2^+$  Nilsson level to survive as a resonant level in the positive-energy region. Nevertheless, we note that a given one-particle resonance with  $\Omega^\pi = 1/2^+$  may survive even at several MeV excitation-energy, if the higher- $\ell$  components are predominant in the wave function inside the potential. In such cases the existence of the resonance is made possible by the presence of the higher- $\ell$  components while the width of the resonance is determined by the small  $\ell = 0$  component.

One-particle resonant levels for spherical shape are defined in terms of phase shift as

described in standard textbooks. On the other hand, the definition of one-particle resonance for deformed potentials is obtained using the eigenphase formalism [1–3]. The definition is a natural extension of the definition of one-particle resonance for spherical potentials in terms of phase shift.

Taking the three bound one-particle levels for neutrons in the  $sd$  shell, in [4] it is shown how the order of the three levels varies as a function of binding energies: from the bottom to the top in energy, (i) the relative level order is  $1d_{5/2}$ ,  $1d_{3/2}$  and  $2s_{1/2}$  for strongly bound cases,; (ii)  $1d_{5/2}$ ,  $2s_{1/2}$  and  $1d_{3/2}$  for about 10 MeV binding and (iii)  $2s_{1/2}$ ,  $1d_{5/2}$  and  $1d_{3/2}$  for very weak bindings. Namely, the  $\ell = 0$  level shifts downwards relative to the  $\ell = 2$  levels, as the potential strength becomes weaker or the binding energy becomes smaller. The level order in (ii) is known as the usual energy splitting in stable  $sd$ -shell nuclei, which is used in the shell model. In the present talk we concentrate on the shell structure of bound and resonant neutron levels in the  $pf$ -shell as well as in the  $50 < N \leq 82$  major shell, taking examples of a stable  $sd$ -shell nucleus (figure 1), a known deformed neutron-drip-line nucleus (figure 2), and a not yet observed neutron-drip-line nucleus in the region of medium mass (figure 3).

## II. MODEL AND NUMERICAL EXAMPLES

In the description of one-particle resonances the formalism using complex energy is sometimes popular in the literature. However, it is equally possible to formulate the resonances using real energy. I prefer to choosing the latter, since the treatment of certain observable quantities such as matrix-elements or wave-function components is much simpler with real variables.

Solving the coupled equations derived from the Schrödinger equation in coordinate space with the correct asymptotic behaviour of wave functions for  $r \rightarrow \infty$ , the shell structure in axially symmetric quadrupole-deformed Woods-Saxon potentials is studied. Whereas one-particle bound levels in the deformed potential are obtained by solving the well-known eigenvalue problem, for positive-energy one-particle levels all eigenphases for a given  $\Omega^\pi$  are calculated, and the possible one-particle resonant level for a given energy  $\varepsilon_\Omega$  and a given  $\Omega^\pi$  value may be identified, which is associated with a particular eigenphase among all possible eigenphases. One-particle resonance is not obtained if none of calculated eigenphases do not

increase through  $\pi/2$  as the one-particle energy increases at the given energy. The relevant formulation can be found in [2, 3].

The parameters of the Woods-Saxon potential are chosen as follows: the diffuseness  $a=0.67$  fm and the radius  $R = r_0 A^{1/3}$  with  $r_0=1.27$  fm, while the depth which depends on the neutron excess in respective nuclei is taken approximately from the expression (2-182) in [5]. The neutron potential for nuclei with a neutron excess is shallower than that for  $N = Z$  nuclei.

#### A. Nilsson diagram for a stable nucleus $^{25}_{12}\text{Mg}_{13}$

The analysis of observed spectroscopic properties of low-lying states in light deformed mirror nuclei,  $^{25}_{12}\text{Mg}_{13}$  and  $^{25}_{13}\text{Al}_{12}$ , in terms of one-particle motion in a deformed potential is very successful [6] using the deformation parameter  $\delta_{osc} \approx 0.4$ . In [6] the Nilsson diagram based on a modified oscillator potential is used. Since the neutron separation energy  $S_n$  of  $^{25}\text{Mg}$  is 7.3 MeV, the properties of low-lying levels could well be described using modified oscillator potential when the related parameters were properly adjusted. In figure 1 the Nilsson diagram based on a deformed Woods-Saxon potential is shown. Observed spectroscopic properties of low-lying states are equally well understood also using the Nilsson diagram in figure 1.

At  $\beta=0$  of figure 1 the  $2s_{1/2}$  level appears around the middle of the  $1d_{5/2}$  and  $1d_{3/2}$  level, as usually assumed. A striking difference of figure 1 from the Nilsson diagram based on the modified oscillator potential (or from one-particle energies used in the conventional shell model) is seen in the energies of the  $2p_{3/2}$  and  $1f_{7/2}$  levels. Calculated one-particle resonant energies are  $\varepsilon_{res}(p_{3/2}) = +0.31$  MeV and  $\varepsilon_{res}(f_{7/2}) = +0.32$  MeV. Namely, the  $p_{3/2}$  level lies even lower than the  $f_{7/2}$  level. In other words, the  $N=28$  energy gap totally disappears in the low-energy resonance spectra.

#### B. Nilsson diagram for a deformed neutron-drip-line nucleus $^{31}_{10}\text{Ne}_{21}$

In figure 2 the Nilsson diagram appropriate for neutrons in  $^{31}_{10}\text{Ne}_{21}$ , of which the measured neutron separation energy  $S_n$  is  $0.29 \pm 1.64$  MeV, is shown. At  $\beta=0$  the  $f_{7/2}$  one-neutron resonance is found at 2.04 MeV, while neither  $p_{3/2}$  nor  $p_{1/2}$  resonance defined by the eigen-

phase formalism is obtained. However, the  $p_{3/2}$  resonance lying clearly lower than the  $f_{7/2}$  resonance is found if we use a slightly more attractive Woods-Saxon potential. The next low-lying one-particle resonant level for  $\beta=0$  is the  $f_{5/2}$  level at 9.50 MeV.

The measured very low excitation-energies of the first  $2^+$  state of both  $^{30}\text{Ne}$  and  $^{32}\text{Ne}$  indicate that the Ne isotope with the neutron numbers is deformed. Furthermore, the large Coulomb breakup cross section reported in [7] clearly suggests the halo nature of the ground state of  $^{31}\text{Ne}$ . In the conventional shell model the 21st neutron for a spherical shape occupies the  $1f_{7/2}$  shell and, thus, the related halo phenomena are impossible to obtain. If  $^{31}\text{Ne}$  is prolately deformed, from figure 2 we obtain the bound Nilsson level which is to be occupied by the 21st neutron having a halo structure:  $[330\ 1/2]$  for  $0.20 \lesssim \beta \lesssim 0.30$  and  $[321\ 3/2]$  for  $0.40 \lesssim \beta \lesssim 0.58$ . In both cases the ground state should have  $3/2^-$  and the  $p$ -wave neutron halo together with the deformed core  $^{30}\text{Ne}$ . The measurement of  $S_n$  with an accuracy which is an order of magnitude better than the presently available one will clarify the intrinsic configuration of the ground state of  $^{31}\text{Ne}$  [8].

Examining figure 2 we may also note that the presence of  $^{31}\text{Ne}$  inside the neutron drip line is possibly realized by the deformation, which is created by the Jahn-Teller effect due to the near degeneracy of  $1f_{7/2}$ ,  $2p_{3/2}$  and  $2p_{1/2}$  shells in the continuum for the spherical shape. Furthermore, it is remarked that the measured magnetic moment of the isotone nucleus  $^{33}_{12}\text{Mg}_{21}$  [9] is in good agreement with the estimated value for the prolately deformed shape [10].

### C. Nilsson diagram for neutron-drip-line nuclei with $A \approx 75$ and $N \approx 50$

In figure 3 the Nilsson diagram appropriate for neutron-drip-line nuclei with  $N \approx 51$  (for example,  $^{75}_{24}\text{Cr}_{51}$ ) is shown. Since in this example the  $1f_{7/2}$ ,  $2p_{3/2}$ ,  $1f_{5/2}$  and  $2p_{1/2}$  levels are well bound, the presence of the magic number  $N = 28$  which is established for stable nuclei is clearly seen. Moreover, the level order of four levels in the  $1f - 2p$  major shell is exactly what is used in traditional shell-model calculations. In contrast, we note the peculiar order of weakly-bound and resonant one-particle levels which belong to the  $50 < N \leq 82$  major shell. At  $\beta = 0$  the very weakly bound  $3s_{1/2}$  level is almost degenerate with (but slightly lower than) the  $2d_{5/2}$  level, and the one-particle resonant levels in the  $50 < N \leq 82$  major shell which are not plotted in the figure are:  $\varepsilon_{res}(1g_{7/2}) = +3.44\text{MeV}$

and  $\varepsilon_{res}(1h_{11/2}) = +5.48\text{MeV}$ . It is noted that the level order in the major shell consisting of the  $3s_{1/2}$ ,  $2d_{3/2}$ ,  $2d_{5/2}$ ,  $1g_{7/2}$ , and  $1h_{11/2}$  levels is totally different from what is known from stable nuclei.

A similarity of the level bunching around  $N=21$  in figure 2 to that around  $N=51$  in figure 3 as a function of deformation is seen especially for  $\beta \geq 0$ . Considering the fact that the  $N=21$  neutron-drip-line nuclei,  $^{31}\text{Ne}$  and  $^{33}\text{Mg}$ , are deformed, the nucleus such as  $^{75}_{24}\text{Cr}_{51}$  may be also deformed, if it indeed lies inside the neutron drip line. In other words, there might be  $N = 51$  nuclei such that they may remain inside the neutron drip line due to the possible deformation. Furthermore, instead of having  $I^\pi = 7/2^+$  or  $5/2^+$  coming from the occupancy of  $1g_{7/2}$  or  $2d_{5/2}$  neutron orbits, respectively, by the 51st neutron the neutron-drip-line nuclei with  $N = 51$  have a good chance to have the ground or very low-lying  $I^\pi = 1/2^+$  state, irrespective of spherical or deformed shape.

### III. SUMMARY AND DISCUSSIONS

It is known that the presence of the surface in realistic potentials of stable nuclei pushes down one-particle levels with higher  $\ell$  relative to lower  $\ell$  levels among the levels belonging to a given major shell of the harmonic-oscillator potential. On the other hand, weakly-bound neutrons with small  $\ell$  have an appreciable probability of being outside the potential compared with those with larger  $\ell$  and thus are insensitive to the strength of the potential. Consequently, those small- $\ell$  levels are pushed down relative to high- $\ell$  levels, as the binding energy becomes small. The resulting shell structure, which is quite different from what we are accustomed to in stable nuclei, would appear in weakly-bound and resonant neutron one-particle levels and affect the nuclear many-body problem in neutron drip line nuclei. In the present talk I have chosen to demonstrate the shell structure of one-particle levels in the  $1f$ - $2p$  shell as well as in the  $50 < N \leq 82$  major shell, when the levels become weakly-bound or resonant. Examining the obtained shell structure one may understand the possible origin of the deformation of nuclei in the island of inversion ( $N \gtrsim 20$ ) as well as a possible deformation of neutron drip line nuclei with  $N \approx 51$ .

The systematic change of shell structure described in the present article is strictly related to the characteristic behavior of the one-particle motion with small orbital angular-momenta. The change cannot be estimated by using harmonic-oscillator potential (or wave function).

In the present meeting the change of shell structure of neutrons (protons) as the proton (neutron) number varies is discussed, considering the tensor force between protons and neutrons using harmonic-oscillator wave functions. Though some of the shell-structure change looks numerically similar to that shown in the present work, the relevant physics is essentially different.

- 
- [1] For example, see; Newton R G 1966 *Scattering Theory of Waves and Particles* (New York: McGraw-Hill)
  - [2] Hamamoto I 2005 *Phys. Rev. C* **72** 024301
  - [3] Hamamoto I 2006 *Phys. Rev. C* **73** 064308
  - [4] Hamamoto I 2010 *J. Phys. G: Nucl. Part. Phys.* **37** 055102
  - [5] Bohr A and Mottelson B R 1969 *Nuclear Structure* vol 1 (New York: Benjamin)
  - [6] Bohr A and Mottelson B R 1975 *Nuclear Structure* vol 2 (New York: Benjamin)
  - [7] Nakamura T et al 2009 *Phys. Rev. Lett.* **103** 262501
  - [8] Hamamoto I 2010 *Phys. Rev. C* **81** 021304(R)
  - [9] Yordanov D T et al 2007 *Phys. Rev. Lett.* **99** 212501
  - [10] Yordanov D T, Blaum K, De Rydt M, Kowalska M, Neugart R, Neyens G and Hamamoto I 2010 *Phys. Rev. Lett.* **104** 129201

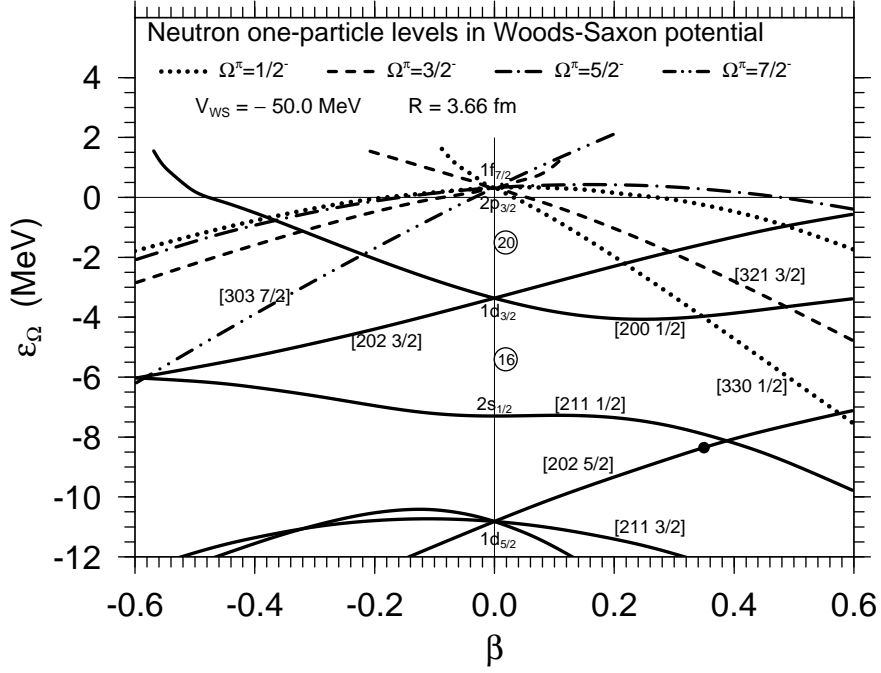


FIG. 1: Neutron one-particle levels as a function of axially-symmetric quadrupole deformation. The depth and radius of the Woods-Saxon potential are designed approximately for  $^{25}_{12}\text{Mg}_{13}$ . The possible occupancy of the 13th neutron in the ground state of  $^{25}\text{Mg}$  is indicated by the filled circle. Some one-particle levels are denoted by the asymptotic quantum numbers,  $[N n_z \Lambda \Omega]$ . One-particle levels plotted for  $\varepsilon_\Omega > 0$  are resonant levels obtained by using the eigenphase formalism, of which the widths are not plotted for simplicity. Note that one-particle resonant  $p_{3/2}$  and  $f_{7/2}$  levels, of which the resonant energies are about 0.3 MeV, are almost degenerate.



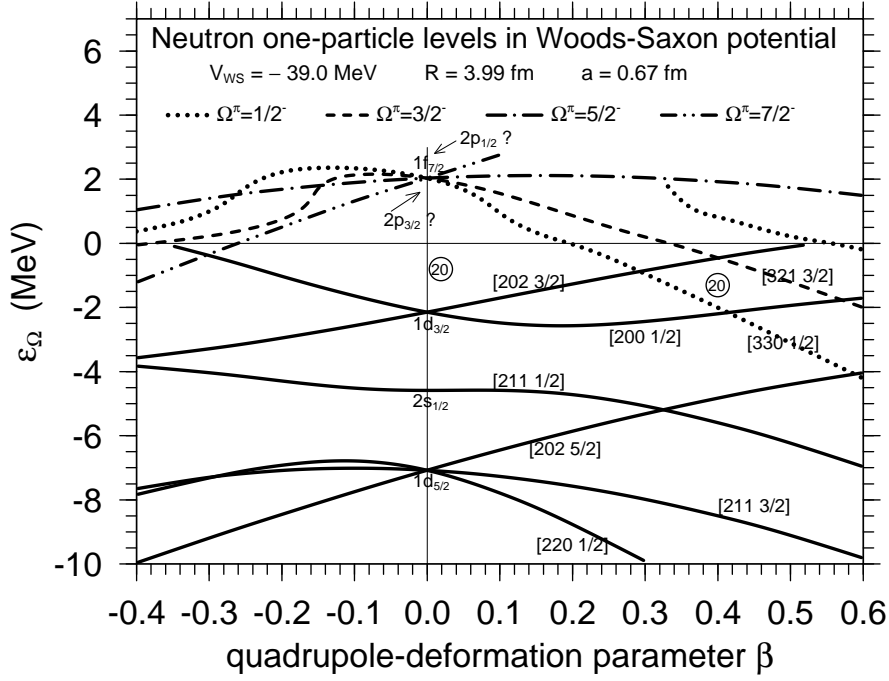


FIG. 2: Neutron one-particle levels as a function of axially-symmetric quadrupole deformation. The depth and radius of the Woods-Saxon potential are designed approximately for  ${}^{31}_{10}\text{Ne}_{21}$ . The neutron number 20, which is obtained by filling in all lower-lying levels, is indicated with a circle. The approximate positions of the  $2p_{3/2}$  and  $2p_{1/2}$  levels for  $\beta = 0$  are indicated with "?", which are extrapolated from the resonant energies obtained by using a slightly more attractive Woods-Saxon potential. For the potential with the present strength the  $p_{3/2}$  and  $p_{1/2}$  resonant levels are not obtained for  $\varepsilon_{\Omega} > 1.3$  MeV, due to the low centrifugal barrier for  $\ell=1$  orbits. The calculated widths of one-particle resonant levels are not plotted, for simplicity.

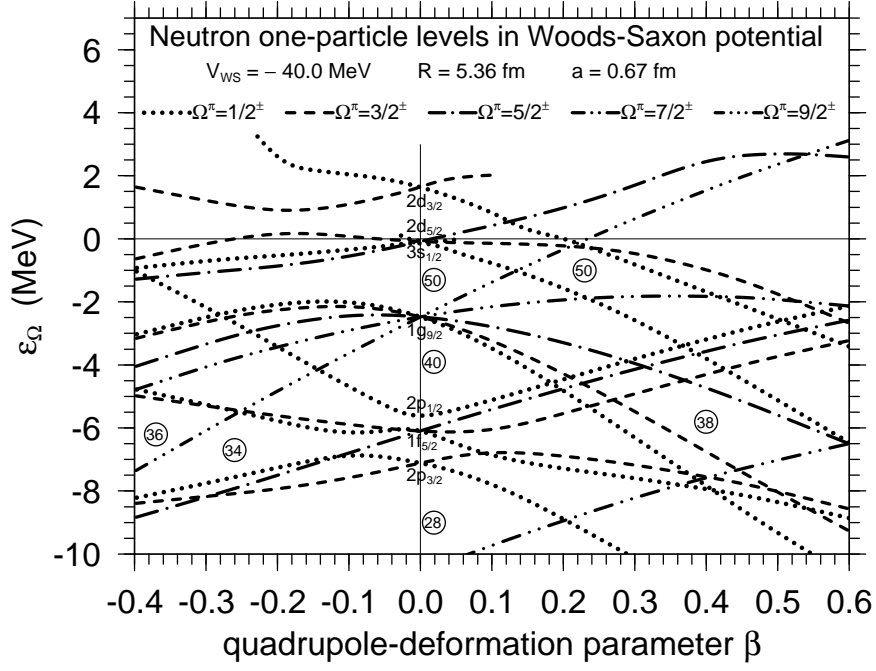


FIG. 3: Neutron one-particle levels as a function of axially-symmetric quadrupole deformation. The depth and radius of the Woods-Saxon potential are designed approximately for  $^{75}_{24}\text{Cr}_{51}$ .